Volume 1 | Number 1 | Jan 2013 | Pages 1–100

Environmental Science

Nano

www.rsc.org/es-nano

ROYAL SOCIETY OF CHEMISTRY

ROYAL SOCIETY OF CHEMISTRY

rsc.li/es-nano

Comparative Life Cycle Assessment of Silver Nanoparticle Synthesis Routes

Leila Pourzahedi and Matthew J. Eckelman[*]

Department of Civil and Environmental Engineering, Northeastern University, 360 Huntington Avenue, Boston, MA 02115, USA

[*] Corresponding Author: m.eckelman@neu.edu, +1 (617) 373 4256

Abstract

Silver nanoparticles (AgNPs) can be produced through a variety of synthesis routes with differing mechanisms, inputs, yields, reaction conditions, and resulting size distributions. Recent work has focused on applying green chemistry and sustainable manufacturing principles to nanomaterial synthesis, with the goal of reducing life cycle energy use and environmental impacts. Life cycle assessment (LCA) is used here to analyze and compare the environmental impacts of AgNPs produced through seven different synthesis routes (cradle-to-gate). LCA reveals both direct and indirect or upstream impacts associated with AgNPs. Synthesis routes were chosen to represent the current trends in nanoparticle synthesis and include physical, chemical and bio-based methods of production. Results show that, across synthesis routes, impacts associated with the upstream production of silver itself were dominant for nearly every category of environmental impact, contributing to over 90% of life cycle burdens in some cases. Flame spray methods were shown to have the highest impacts while chemical reduction methods were generally preferred when AgNPs were compared on a mass basis. The bio-based chemical reduction route was found to have important tradeoffs in ozone depletion potential and ecotoxicity. Rescaling results by the size-dependent antimicrobial efficacy that reflects the actual function of AgNPs in most products provided a performance-based comparison and changed the rank order of preference in every impact category. Comparative results were also presented in the context of a nanosilver-doped wound dressing, showing that the overall environmental burdens of the product are highly sensitive to the synthesis route by which the AgNPs are produced.

32

Keywords

34   engineered nanomaterials; nanosilver; green synthesis; nanomanufacturing; environmental

35   assessment

Environmental Science: Nano

36 ## 1. Introduction

37 Silver nanoparticles (AgNPs) are a versatile class of engineered nanomaterials (ENMs),

38 produced in the hundreds of tons annually and used in a wide range of consumer and high-tech

39 products. Major end-uses categories include medical products (30%), paints and coatings (25%),

40 textiles (15%), and cosmetics (15%).[1] Silver has the highest electrical and thermal conductivity

41 and reflectivity of all the elements, but the function of AgNPs in the majority of applications

42 currently is as an antimicrobial agent. Antimicrobial activity of AgNPs is a function of particle

43 morphology and surface chemistry, as well as environmental conditions including ionic strength

44 and the presence of natural organic matter (NOM).[2]

45

46 Increasing commercial production volumes of ENMs generally has led to extensive research into

47 potential environmental and health implications of their use, particularly given the projections

48 for their widespread incorporation into consumer products. This research includes mechanisms

49 and projected magnitudes of ENM releases from products,[3,4] treatment and control technology

50 efficiencies,[5,6] fate and transport in the environment,[2,7,8] and potential exposures and effects.[9–11]

51 Based on a mechanistic understanding of ENM fate and effects, research is also increasingly

52 being directed at the design of ENMs that mitigate environmental exposures and potential toxic

53 effects, for example through addition of surface functional groups.[12] In the case of AgNPs,

54 considerations of impact have centered on ecotoxicity to aquatic organisms. Thousands of tons of

55 silver compounds are estimated to be released worldwide to the environment annually, only a

56 fraction of which is nanosilver, but their impacts vary widely across the different chemical and

57 physical forms of the emissions.[13]

58

59 In addition to releases of ENMs themselves, the resource intensity of nanomaterial synthesis has

60 also been identified as of environmental concern. Production of nanomaterials can be orders of

61 magnitude more energy- and materials-intensive than for fine chemicals or pharmaceuticals,[14]

62 often with low yields and involving toxic or hazardous reagents and solvents.[15] Life cycle

63 assessment (LCA) studies of ENMs that consider the environmental implications across

64 production, use, and release have found that energy and chemicals use during ENM synthesis

65 contributes a significant, and often dominant share of total life cycle environmental impacts.[16,17]

66 In earlier work, we reported LCA results for a medical bandage treated with AgNPs synthesized

67   via magnetron sputtering, examining the relative contribution of AgNPs to the life cycle impacts

68   of bandage production and end-of-life incineration.[18] The production of AgNPs was the largest

69   contributor to product impacts across all environmental categories, despite low concentrations in

70   the bandage. These impacts were driven by extraction and processing of the silver, as well as

71   synthesis-related resource inputs, particularly electricity.

72

73   Metallic nanoparticles such as gold and silver can be synthesized using a wide variety of

74   techniques, including vapor deposition, ablation and sputtering, flame spray pyrolysis,

75   electrochemical methods, microwaves, and chemical reduction methods.[15,19] Green chemistry

76   and green nanoscience researchers have been successful at developing novel synthesis routes that

77   reduce resource requirements and use benign chemicals, while maintaining control of ENM size

78   and morphology.[20]

79

80   Given the importance of synthesis processes to life cycle impacts of ENMs, using synthesis-

81   specific life cycle data is critical to achieving accurate LCA results for existing nano-enabled

82   products. Unfortunately, representative and validated life cycle inventory data are lacking for

83   many nanoparticle synthesis methods that have been reported in the literature, and there have

84   been calls to accelerate efforts to make these data sets available.[21] In addition, most nano LCA

85   studies have considered only a single synthesis method, yet comparisons across synthesis routes

86   can also identify drivers of overall impacts and the relative environmental advantages of a certain

87   route, complementing other considerations of purity, yield, and cost.[16,22,23] For example, a recent

88   article by Pati et al. compared chemical reduction routes for the synthesis of gold nanoparticles

89   using 3 conventional and 13 bio-based reducing agents.[24] Gold itself was the most important

90   driver of life cycle energy use, such that syntheses using bio-based reducing agents but with low

91   yields and long reaction times were not favored. Such information can also be used to prioritize

92   research for improving novel synthesis routes prior to commercial scale-up.

93

94   Here we present life cycle inventory data and detailed assessment results for seven AgNP

95   synthesis routes (including one bio-based route) in order to compare the magnitude and patterns

96   of impacts across multiple environmental categories. AgNPs produced through different routes

97   have varying size distributions and morphologies, and so results are presented both per unit mass

98 and also normalized by their estimated antimicrobial efficacy. These data and results are

99 intended for use in further research into ENM synthesis as well as subsequent environmental

100 assessments of AgNP-enabled products.

101

2. Methods and Modeling

2.1 Scope and System Boundary

104 This cradle-to-gate analysis considers the direct emissions from AgNP production and indirect

105 impacts associated with upstream resource extraction and energy generation. Production methods

106 of seven different nanosilver synthesis routes and their corresponding material and energy inputs

107 are described in Section 2.2. Environmental impacts were analyzed and compared initially using

108 a mass-based functional unit of 1 kg of AgNPs, and later normalized by their estimated

109 antimicrobial efficacies (Section 2.3). Additionally, potential impacts of AgNPs were studied in

110 context of a commercial product, Acticoat 7, a commercially available medical bandage

111 containing nanosilver. Life cycle inventory data for this product can be found in our earlier

112 work.[25] Here we model the relative contribution of AgNPs to the overall product, considering

113 each of the modeled AgNP synthesis routes.

114

2.2 AgNP Synthesis Routes

116 The AgNP methods of production considered here can be classified into two general categories:

117 wet chemistry and physical techniques. Wet chemistry through chemical reduction utilizes

118 solutions of silver reacted with an appropriate reducing agent to produce metallic nanoparticles,

119 while capping agents are typically added to stabilize the colloidal solution. Here, reduction of

120 silver nitrate with trisodium citrate (CR-TSC),[26] sodium borohydride (CR-SB),[27] and ethylene

121 glycol (CR-EG) were considered.[28] Chemical reduction of silver nitrate with soluble starch from

122 potatoes (CR-Starch) was also modeled in this study as a representative, novel bio-based

123 chemical reduction method,[29] though citric acid for the CR-TSC method is also industrially

124 produced through biotechnological means. Material input was based on data provided by the

125 literature. Energy required for heating solutions was calculated based on the heat capacity of

126 water. Physical routes considered in this were flame spray pyrolysis (FSP),[16] arc plasma (AP),[30]

127 and reactive magnetron sputtering with an argon and nitrogen gas mixture (RMS-AR-N).[31]

128 Further details and life cycle inventory (LCI) data for all methods can be found in the

129 subsections below and Tables S1-S7 of the SI. A summary of all methods and their resulting

130 particle size ranges is provided in Table 1.

131

2.2.1 Chemical Reduction of Silver Nitrate with Trisodium Citrate (CR-

133 **TSC)**

134 Synthesis of citrate-stabilized nanosilver was first reported in 1889.[32] The method considered

135 here reduces a 1 mM silver nitrate solution using 1% trisodium citrate. The process reaction is as

136 follows,[26]

137 $$4\ Ag^+ + C_6H_5O_7Na_3 + 2\ H_2O \rightarrow 4\ Ag^0 + C_6H_5O_7H_3 + 3Na^+ + H^+ + O_2\uparrow$$
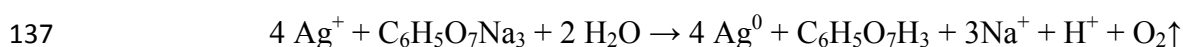
138 To simulate this reaction, chemical elements must not be in their ionized form, hence it is

139 assumed that the previous reaction is a result of the reaction below,

140 $$12\ AgNO_3 + 4\ C_6H_5O_7Na_3 + 10\ H_2O \rightarrow 12\ Ag + 4\ C_6H_5O_7H_3 + 12\ NaNO_3 + 4\ H_2 + 5\ O_2$$
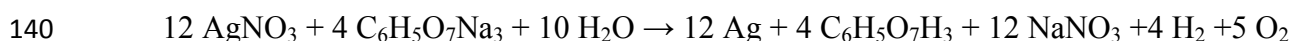
141 Silver nitrate is heated to boiling prior to the addition of trisodium citrate. The mixture is further

142 heated until the formation of AgNPs. Stoichiometric relations suggest that, production of 1 kg

143 AgNPs from this reduction requires 1.57 kg silver nitrate, 0.8 kg trisodium citrate, and 0.14 liter

144 of water. Byproducts of this reaction are 0.6 kg citric acid, 0.8 kg sodium nitrate, 0.006 kg

145 hydrogen gas and 0.12 kg oxygen. The minimum heating energy required to boil the solution

146 was calculated based on the heat capacity of the solution.

147 Production of trisodium citrate was studied as part of this synthesis route. One kg of this

148 compound is obtained by reacting 0.74 kg citric acid with 0.46 kg sodium hydroxide, as per the

149 chemical reaction assumed below (0.2 liter water is also produced alongside trisodium citrate),

150 $$C_6H_8O_7 + 3\ NaOH \rightarrow Na_3C_6H_5O_7 + 3\ H_2O$$

151 Citric acid is industrially manufactured using the fungus *Aspergillus niger* and a source of sugar.

152 This is done by a submerged fermentation technique. Here, sugarcane was used as the source of

153 sugar. The reaction below shows the process performed by the fungus, in which 0.93 kg glucose

154 is needed to produce 1 kg citric acid,[33]

155
$$C_6H_{12}O_6 + 3/2\ O_2 \rightarrow C_6H_8O_7 + 2\ H_2O$$

156 After this step, citric acid is treated with calcium hydroxide and sulfuric acid for further
157 purification, reactions shown below,[34]

158
$$3\ Ca(OH)_2 + 2\ C_6H_8O_7 \rightarrow Ca_3(C_6H_5O_7)_2\ .\ 4\ H_2O + 2\ H_2O$$

159
$$3\ H_2SO_4 + Ca_3(C_6H_5O_7)_2\ .\ 4\ H_2O \rightarrow 2\ C_6H_8O_7 + 3\ CaSO_4\ .\ 2\ H_2O + 2\ H_2O$$

160 Treatment of 1 kg citric acid requires 0.76 kg sulfuric acid and 0.57 kg calcium hydroxide
161 (hydrated lime). Hydrogen and calcium sulfate (gypsum) are both by-products of these reactions.
162

2.2.2 Chemical Reduction of Silver Nitrate with Sodium Borohydride
(CR-SB)

165 Reducing silver salt solutions with sodium borohydride is the most common method used among
166 chemical reduction syntheses.[35] The reduction of a 1 mM silver nitrate solution with a 2 mM
167 sodium borohydride solution was considered based on the reaction below,[27]

168
$$AgNO_3 + NaBH_4 \rightarrow Ag + \tfrac{1}{2}\ H_2 + \tfrac{1}{2}\ B_2H_6 + NaNO_3$$

169 Due to the exothermic nature of this process, sodium borohydride is chilled in an ice bath prior to
170 the addition of silver nitrate, in order to decrease the rate of reaction. As sodium borohydride
171 undergoes side reactions during silver nitrate reduction, it is generally used in excess.[27] The
172 molar ratio of sodium borohydride to silver nitrate directly affects the rate of formation of
173 AgNPs, with a range of ratios reported.[27,36,37] Any unreacted sodium borohydride that could be
174 recovered and recycled would be subtracted from the life cycle inventory. Therefore, as a
175 baseline the above reaction was used here to calculate the stoichiometric amount of $NaBH_4$
176 needed to reduce silver nitrate. 1.57 kg silver nitrate and 0.35 kg sodium borohydride are needed
177 to obtain 1 kg silver particles alongside 0.12 kg diborane, 0.78 kg sodium nitrate and 0.009 kg
178 hydrogen as emissions and co-products. Production of Sodium borohydride was further studied.
179 Sodium borohydride is produced by reacting 2.27 kg trimethyl borate and 2.5 kg sodium hydride.
180 The aforementioned amounts result in 1 kg sodium borohydride and 4.28 kg sodium methoxide
181 as a co-product. Below is the chemical reaction for this process,[38]

182 $$B(OCH_3)_3 + 4\,NaH \rightarrow NaBH_4 + 3\,NaOCH_3$$

183 Here, sodium hydride was modeled using inventory data for sodium hydroxide, as both are
184 produced by electrolysis of sodium chloride.

185

186 2.2.3 Chemical Reduction of Silver Nitrate with Ethylene Glycol (CR-
187 EG)

188 In this technique, ethylene glycol is used as the reducing agent to obtain silver particles from
189 silver nitrate (with 3.81 g/L silver concentration) and poly *n*-vinylpyrrolidone (PVP) is used as
190 the stabilizing agent.[39] The reaction takes place at room temperature.[39–41] For the production of 1
191 kg silver particles, 1.57 kg silver nitrate, 291 kg ethylene glycol and 47 kg PVP are required. A
192 recycling rate of 90% was assumed for ethylene glycol, consistent with most LCI datasets for
193 chemicals, thus only 29.1 kg of this product is required as input per kg AgNPs.

194

195 To produce PVP, first 1,4-butanediol is dehydrogenated over copper at 200°C to form gamma-
196 butyrolactone. Gamma-butyrolactone is then reacted with ammonia to obtain pyrrolidone, which
197 is subsequently treated with acetylene yielding VP monomers. Reactions below describe these
198 set of processes,[42]

199 $$C_4H_{10}O_2 \rightarrow C_4H_6O_2 + 2\,H_2$$

200 $$C_4H_6O_2 + NH_3 \rightarrow C_4H_7NO + H_2O$$

201 $$C_4H_7NO + C_2H_2 \rightarrow C_6H_0NO$$

202 Stoichiometric relations require that for producing 1 kg PVP, 0.8 kg 1,4-butanediol, 0.15 kg
203 ammonia and 0.23 kg acetylene is required. Emissions from these reactions were calculated to be
204 0.04 kg hydrogen and 0.16 liter water.

205

206 2.2.4 Green Synthesis using Soluble Starch (CR-Starch)

207 To reduce life cycle impacts due to the chemical reducing agents, plant extracts can be used as an
208 bio-based alternative.[43] Here we consider synthesis of AgNPs using a starch solution as both the
209 reducing and stabilizing agent for the silver nitrate solution.[29] Here, 0.9 g of a chemically

210   modified starch (hydroxypropyl starch, with molar substitution ratio of 0.84, resulting in its

211   complete solubility in water) is added to 100 ml deionized water and heated up to 70°C. The

212   dissolved starch solution is used to reduce the silver nitrate solution. An AgNP solution with a

213   concentration of 100 ppm was formed after 60 minutes of heating. The heat required to bring the

214   solution up to temperature was subsequently calculated. With ~100% yield,[44] to produce 1 kg of

215   silver nano particles, 90 kg of starch is required alongside 1000 liter of water to reduce 1.57 kg

216   of silver nitrate.

217

218   2.2.5 Flame Spray Pyrolysis (FSP), Utilizing a Methane-Oxygen Flame

219   This technique produces nano-particles of metal or metal oxides by combusting metal precursor

220   solutions. The particles are formed just above the flame and collected from a filter.[16] Here, a

221   precursor solution of silver octanoate was sprayed into a methane-oxygen flame.[16] Producing 1

222   kg of pure silver nano-particles using this route requires 33.4 kg oxygen, 1.53 kg methane, 62.8

223   liter water, 2.35 kg silver octanoate, 6.29 kg 2-ethylhexanoic acid, 6.29 kg xylene, and 25.1 kWh

224   of electricity.

225   In addition, silver octanoate and 2-ethylhexanoic acid lacked existing LCI data and so were

226   modeled separately. To produce 1 kg of 2-ethylhexanoic acid, 1.02 kg *n*-butyraldehyde is

227   needed, while 0.05 kg CO_2 emissions and 7 g of steam are generated as byproducts. N-

228   butyraldehyde is an organic compound, commercially manufactured using the oxo process,

229   where propylene, carbon monoxide and hydrogen are combined with in the presence of a

230   rhodium or cobalt catalyst,[16]

231    $$2\ CH_3CH=CH_2 + 2\ CO + 2\ H_2 \rightarrow CH_3(CH_2)_2CHO + (CH_3)_2(CH)_2O$$

232   From propylene, *n*- and iso-butyraldehyde are produced. This reaction gives a 4:1 ratio of *n*- to

233   iso-butyraldehyde.[16] Following Walser et al., we use an economic allocation factor of 90% to

234   assign process burdens to the *n*-butyraldehyde. By this reaction, manufacturing 1 kg *n*-

235   butyraldehyde requires 0.58 kg propylene, 0.02 kg oxygen, and 0.39 kg carbon monoxide.

236   Silver octanoate is derived from the reaction between octanoic acid (a fatty acid component of

237   coconut oil), silver nitrate, sodium hydroxide, and deionized water.[16] To obtain 1 kg of silver

238   octanoate, 2.7 kg crude coconut oil, 2.57 kg silver nitrate, 0.38 kg sodium hydroxide, and 0.9

239 liter deionized water are required. Silver nitrate is commercially produced by dissolving silver

240 metal in cold and diluted nitric acid in a pure oxygen environment. This process produces

241 nitrogen monoxide and water as a result of the oxidation, chemical reaction shown below,[45]

242 $$3\,Ag + 4\,HNO_3 \rightarrow 3\,AgNO_3 + 2\,H_2O + NO$$
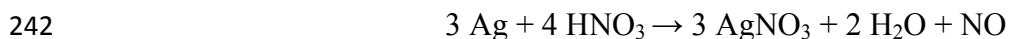
243 Based on this stoichiometry, to produce 1 kg of silver nitrate, 0.49 kg nitric acid and 0.64 kg

244 silver are needed. In this process 0.07 liter water and 0.06 kg nitrogen monoxide are also

245 produced as byproducts.

246

247 2.2.6 Arc Plasma Reactor (AP)

248 Arc Plasma is a physical vapor deposition method modeled in this study.[30] Particles are created

249 by vaporizing pure silver in a reactor using a high electricity discharge. They are then condensed

250 in an argon chamber, simultaneously depositing onto the substrate with a rate of 1.2 g/min.

251 Based on previous studies, an average argon flow rate of 5 l/min was assumed here.[46,47]

252 Assuming 100% yield, to produce 1 kg of silver nano-particles, 1 kg of pure silver, 7.4 kg of

253 argon gas and is required using a DC current of 120 A with a voltage of 25 V.

254

255 2.2.7 Reactive Magnetron Sputtering of Silver with Ar-N$_2$ Gas Mixture
256 (RMS-AR-N)

257 Reactive magnetron sputtering (RMS) is another type of physical vapor deposition. This process

258 uses argon as an inert gas for bombardment of the sputtering target, silver. The collision results

259 in the ejection of silver ions and their movement toward the substrate. In reactive sputtering, a

260 mixture of argon and reactive gases is used to deposit films of oxide or nitride forms of the target

261 onto the substrate surface. Here, material and energy consumption for producing 1 kg of AgNPs

262 were estimated based on experimental data for an argon-nitrogen gas mixtures.[31] To produce 1

263 kg of AgNPs from 1 kg pure silver (assuming 100% yield), 10.4 g nitrogen gas and 124 g argon

264 is required and 27.8 kWh of electricity is used for this process.

265

266 **Table 1.** Synthesis route summary and particle size distribution.

Synthesis	Mechanism	Source of	Abbreviation	Size	Source

Category		Silver		(nm)	
Wet Chemistry	Reduction with trisodium citrate	AgNO₃	CR-TSC	100	Sileikaite *et al.*[26]
	Reduction with sodium borohydride		CR-SB	1-100	Mulfinger *et al.*[27]
	Reduction with ethylene glycol		CR-EG	10.4	Slistan-Grijalva *et al.*[39]
	Reduction with soluble starch		CR-Starch	10-34	El-Rafie *et al.*[29]
Physical Routes	Flame spray pyrolysis	AgC₈H₁₅O₂	FSP	1-2	Walser *et al.*[16]
	Arc plasma	Ag₍ₛ₎	AP	20-100	Zhou *et al.*[30]
	Reactive magnetron sputtering in Ar-N₂	Ag₍ₛ₎	RMS-AR-N	50-60	Pierson *et al.*[31]

267

268

2.3 AgNP Functional Unit

Functional unit is a central consideration in life cycle assessment and other comparative analytical techniques. The antimicrobial efficacy of AgNPs in products depends on characteristics such as particle size, shape and capping agent, as well as how the AgNPs are incorporated.[48,49] As shown in Table 1, the various synthesis routes considered here can produce particles over a wide size range. Nanoparticle size and shape can be tuned by controlling reaction conditions, depending on synthesis route. In the FSP method, the concentration of the metal precursor and the rate at which it is fed to the spray gun affect the particle size.[50] In the arc plasma technique, higher arc current results in larger particle sizes.[51] As the evaporation rate of the precursor metal increases the size of silver particles and the standard deviation of their size distribution also increases.[46] For chemical reduction methods, the size and shape of the particles are affected by the type of stabilizing agent, reducing agent and its redox potential, molar ratios, and other conditions of the experiment.[52] Ordinarily, the particles formed via chemical reduction have higher impurity levels (depending on the reducing efficiency) than other methods but are capable of producing homogenous nanoparticles with regular shapes.[52] Even though green synthesis routes use the same chemical reduction techniques, there is typically less control over the size of particles when using bio-based reducing agents.[52]

To account for properties and characteristics of nanoparticles, as an alternate functional unit to 1 kg AgNP production, the bioactivity of AgNPs was explored in the form of LC_{50}. This is the lethal concentration where 50% loss of the sample population is observed. Antimicrobial

289 efficacy of AgNPs produced by each method were estimated using size-dependent LC_{50} values

290 (µg/ml).[53] A linear regression was obtained using experimental toxicity data for zebrafish

291 embryos subjected to a range of nanosilver particle sizes:

292 $$LC_{50} \approx 0.6D + 18; \; R^2 = 0.41,$$

293 where D is the diameter of the nanoparticles (in nm). In general, larger particles require higher

294 concentrations to kill 50% of the population, illustrating the potency of AgNPs smaller in size.

295 Only relative values are required, and it is assumed here that nanosilver will display the same

296 size-dependent toxicity trend for bacteria.

297

298

299

300 ## 2.4 Life Cycle Assessment Modeling

301 Analysis of life cycle impacts was performed using SimaPro 8.1 as the modeling platform. Each

302 record of energy and chemical use derived in Section 2.2 was matched with an appropriate unit

303 process from the US-EI database, the Ecoinvent 3.1 database adjusted for U.S. energy inputs.

304 Environmental impacts were modeled using the U.S. EPA's Tool for the Reduction and

305 Assessment of Chemical and Other Environmental Impacts (TRACI) 2.1 assessment method.[54]

306 This method considers the impact categories of global warming potential (kg CO_2 equivalents

307 [eq]), ozone depletion (kg CFC-11 eq), smog formation (kg O_3 eq), respiratory effects (kg PM_{10}

308 eq), acidification (mol H^+ eq), eutrophication (kg N eq), human health impacts from toxic

309 carcinogenic and noncarcinogenic substances (health comparative toxic units, or CTUh), and

310 ecotoxicity (CTUe). Detailed life cycle inventory, and additional process contribution analysis

311 for synthesis routes can be found in the Supporting Information (SI). Tables S1 to S7 include the

312 full life cycle inventory from synthesis route modeling.

3. Comparative Results and Discussion

Results and discussion for this analysis have been organized into five sections. Section 3.1 discusses the comparative environmental impact assessment on a mass basis between the synthesis routes. Section 3.2 considers the rescaling of the previous comparative results for the functional unit. Processes contributing to the overall impacts of production are explained in Section 3.3. Comparison of the findings of this study to LCAs previously performed on AgNPs is discussed in Section 3.4. Finally, Section 3.5 demonstrates the effect of synthesis choice in the context of a nano-enabled product. Figures S1 to S7 of the Supporting Information illustrate the LCA results for each synthesis route and the relative contribution of their components. A comparative mass-based LCA of the reducing agents used in this study is shown in Figure S8. Figures S9 and S10 clarify the main contributors of global warming and ecotoxicity impacts of silver itself.

3.1 Synthesis Comparison by Mass

Comparison among synthesis routes was first performed using a mass-based functional unit of 1 kg of AgNPs, with relative results shown in Figure 1a (absolute values can be found in Table S8). Analysis indicates that manufacturing silver particles using the flame spray pyrolysis method with silver octanoate as the precursor sprayed in a methane-oxygen flame has the highest of impacts across all categories except fossil fuel use. These relatively high impacts are largely due to the low AgNP production yield of the FSP synthesis route (roughly 50%) relative to other routes, as well as significant direct electricity use (see Table S5 and Figure S5). Yield has been shown in several previous reports to drive environmental impacts,[24] because life cycle assessments account for all of the energy and materials used to produce reagents, including those that are used in excess.

Chemical reduction with ethylene glycol had the highest level of fossil fuel use overall, due to the substantial use of fossil-based ethylene in upstream chemical production. Just among chemical reduction methods, CR-EG had the highest impacts for smog, carcinogenics, and fossil fuel depletion impact categories. This is due both to the silver precursor and to the reagents used, especially EG and the PVP used as a capping agent. On a unit mass basis, the life cycle environmental impacts of ethylene glycol are modest when compared to other reducing agents,

13

343   with the highest relative impacts in the categories of acidification and respiratory disease, where

344   volatilized ethylene glycol acts as a precursor to secondary particulate matter (see Figure S8).

345   But as ethylene glycol is being used in large quantities for this chemical reduction route (29.1

346   kg/kg AgNPs), the upstream production of chemicals drives impacts in most categories for this

347   synthesis route. Reduction with trisodium citrate dominates for global warming potential as the

348   reaction is carried out at boiling temperature, requiring comparatively more heating energy

349   compared to other chemical reduction methods, which in turn results in higher GHG emissions.

350

351   Again among chemical reduction methods, CR-Starch had the highest impacts for ozone

352   depletion, acidification, eutrophication, non-carcinogenics and ecotoxicity, despite using bio-

353   based reagents. Ozone depletion potential for this bio-based route is due to the use of

354   trichloromethane in pesticides for potatoes, while runoff of fertilizers and pesticides causes

355   higher eutrophication and ecotoxicity impacts compared to conventional chemical reduction

356   methods. These results are also highly dependent on the temperature at which the reaction

357   occurs. For comparison, the method described in Section 2.2.4 was compared to another CR-

358   Starch report which used an autoclave to increase the reaction temperature to $121°C$ at 15 psi

359   (103.4 kPa).[55] Discussion of these results (Figure S9) can be found in Section 1 of the SI. This

360   result emphasizes that the use of bio-based solutions will not necessarily result in reduction of

361   impacts on a life cycle basis and thorough analyses are required prior to adopting alternative

362   synthesis methods

363

364   Finally, reduction with sodium borohydride was shown to have the lowest impact levels despite

365   the high impacts per unit mass from producing sodium borohydride compared to other reducing

366   agents. Modeling sodium borohydride inputs in excess ($3\times$ stoichiometric requirements) does

367   not noticeably change these results.

368

369   **3.2 Syntheses Comparison by Particle Size/Function**

370   Using mass as a basis for comparison ignores performance differences among AgNPs produced

371   through these various synthesis routes. Figure 1b shows the comparative results rescaled with

372   respect to their size-dependent toxicity (LC_{50}) levels. Even though CR-TSC AgNPs had

373   relatively low levels of impact per kg of synthesized particles, in Figure 1b they are revealed to

374   have the highest impacts in all categories. As reported, CR-TSC AgNPs had larger diameters

375   (100 nm) and thus smaller surface-to-volume ratios than AgNPs synthesized through other

376   means, such that more of these particles are required in order to perform the same antimicrobial

377   functionality as particles with smaller diameter (killing 50% of the bacterial population). High

378   mass-based impact values for FSP and CR-Starch resulted in these routes being the second most

379   impactful after rescaling by function. These rescaled results are sensitive to the average particle

380   sizes assumed for each synthesis route. In reality, AgNP size can be controlled by varying

381   reaction conditions or inputs, depending on the synthesis route. It may be possible for a single

382   route to produce AgNPs of different sizes with only marginally different mass-based results but

383   with appreciably different function-based results. Here we rely on a single size value for each

384   route to demonstrate that function-based results (as all LCA results should be) shown in Figure

385   1b depend both on the environmental burdens of production and the bioactivity of the

386   nanoparticles.   These results are specific to antimicrobial products; results for other product

387   categories would have to be rescaled separately according to their primary function.
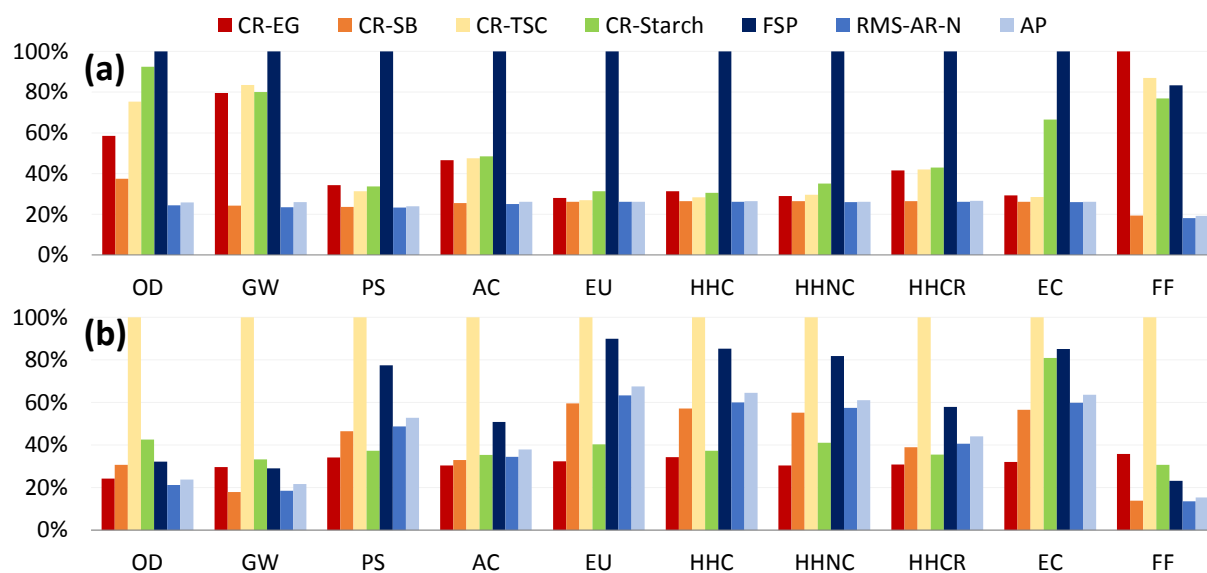
389   **Figure 1.** Relative environmental impacts of multiple AgNP synthesis routes (a) TRACI 2.1 life cycle
390   impact assessment method, (b) re-scaled impacts with respect to size-dependent bioactivity
391   *Abbreviations*: chemical reduction with trisodium citrate (CR-TSC), chemical reduction with sodium
392   borohydride (CR-SB), chemical reduction with ethylene glycol (CR-EG), chemical reduction with soluble
393   starch (CR-Starch), flame spray pyrolysis (FSP), arc plasma (AP); potential impact categories are ozone
394   depletion (OD), global warming (GW), photochemical smog (PS), acidification (AC), eutrophication
395   (EU), human health: carcinogens (HHC), human health: non-carcinogens (HHNC), human health: criteria
396   air pollutants (HHCR), ecotoxicity (EC), fossil fuel depletion (FF).

397

398

3.3 Analysis of Process Contribution

400 In order to show which inputs and processes are contributing most to impacts in each category,
401 detailed results are shown for two synthesis routes in Figure 2: FSP and CR-Starch, representing
402 physical and chemical methods, respectively. CR-Starch is highlighted as well to explore the
403 significance of using a bio-based reducing agent. Corresponding figures for all other routes are
404 provided in the SI. For all routes, the contribution of the source of silver (in most cases silver
405 nitrate) is much greater than the other chemical inputs. This is largely due to industrial activity
406 involved in the mining and refining of silver and its transport (commonly by air). In terms of
407 ecotoxicity, the impacts stem from result from leaching of mining tailings (Figures S10 and S11).
408 These results mirror that found for gold nanoparticles by Pati *et al*. and suggests that life cycle
409 impacts from precious metal nanoparticle synthesis can be most effectively reduced by
410 improving synthesis yields and recovering silver from spent solutions. Additionally, synthesis
411 routes that use bio-based reducing agents but sacrifice nanoparticle yields may end up increasing
412 environmental impact overall.[24]

413 For the case of FSP, as seen in Figure 2a, an analysis of process contributions demonstrates that
414 nearly 80% of the GHG emissions result from upstream industrial energy use, including
415 combustion of coal for electricity and diesel for transportation; only 10% of global warming
416 impact is due to the flame used in the synthesis process itself. For soluble starch reduction,
417 Figure 2b illustrates that the contribution of the starch solution ranges from as low as 10% to
418 carcinogenics up to 60% to ecotoxicity. It is important to note that, while potato starch is benign
419 compared to more toxic chemical reducing agents, indirect toxicity impacts occur during potato
420 cultivation from the runoff of pesticides and herbicides and their subsequent ecotoxic and
421 eutrophic effects. Perhaps surprisingly, production of deionized water also results in noticeable
422 impacts, particularly for ozone depletion from trichloromethane used in the production of anionic
423 resins. For global warming potential and fossil fuel depletion, energy use contributes to more
424 than 50% of the impacts.
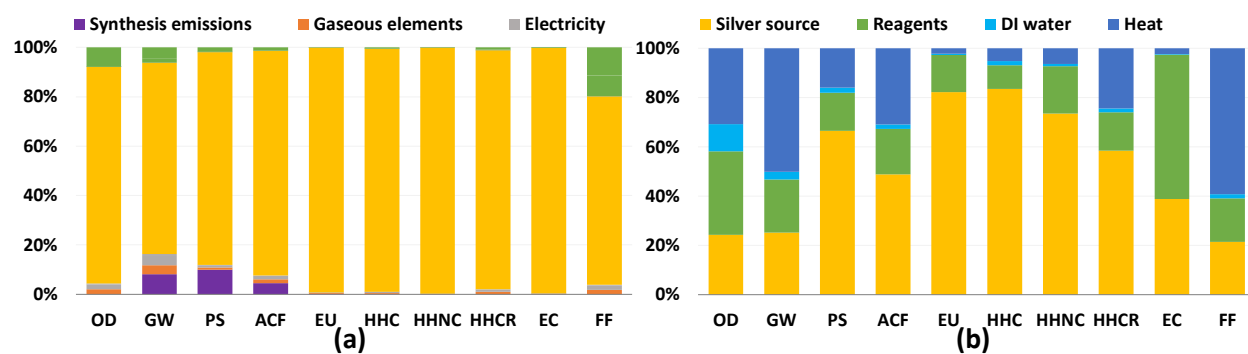
Figure 2. (a) Process contribution for all TRACI impact categories of FSP synthesis route (silver source is silver octanoate, reagents are 2-ethylhexanoic acid and xylene, gaseous elements are oxygen and methane). (b) Process contribution for all TRACI impact categories of bio-based synthesis route (silver source is silver nitrate, reagent is soluble starch solution).

3.4 Comparison to Previous Results

A previous screening-level LCA performed on AgNP-enabled socks also compared a flame spray pyrolysis and arc plasma method, as well as an undisclosed CR route, using an Economic Input-Output (EIO) LCA model.[22] It should be noted here that process-based (used here) and EIO LCA models are different in structure and scope. The former is a bottom-up engineering model while the latter is a top-down economic model, with production of goods aggregated into broad economic sectors. Unlike process-LCA where chemical and energy inputs can be specified individually and in physical units, in EIO-LCA there is a single sector input for silver, gold, and other precious and non-ferrous metals. In spite of these model differences, comparison of our results with those of Meyer *et al.* show the same relative pattern across all impact categories: FSP having higher impact levels than AP and chemical reduction having the lowest impacts among synthesis methods.

3.5 Impact Assessment in Context of Products

A final analysis was performed as an extension to previous work on nano-enabled bandages.[18] Previous findings for the specific AgNP synthesis route used for the Acticoat 7 product, RMS-AR-N, showed the upstream electricity production dominated the global warming impacts of synthesis and that mining emissions dominated ecotoxicity impacts. Here, we present the range of product-level results for these two impact categories when the exact synthesis route is not

450 known. Figure 3 represents the absolute potential global warming and ecotoxicity impact results

451 for a 10 × 12.5 cm^2 piece of Acticoat 7 bandage (material components of this bandage can be

452 found in Table S9). The contribution of AgNPs to product-level impacts is shown as the average

453 for all synthesis routes, while the error bars represent the AgNPs produced through the most- and

454 least- impactful synthesis routes. Physical synthesis routes directly deposit the AgNPs onto the

455 substrate with no extra energy requirements. For the chemical synthesis methods, dip coating of

456 the substrate by submerging it into the final AgNP solution was assumed. Pad-dry-cure

457 techniques have been reported for coating textiles with nanoparticles.[56,57] Figure 3 illustrates

458 dominant contribution of AgNPs to product life cycle impacts, regardless of how they are

459 produced and despite being incorporated into the bandage at low loading levels. These results

460 also show the sensitivity of the overall impacts of the bandage to the method of nanoparticle

461 synthesis, again underlining the importance for product manufacturers and researchers of using

462 synthesis-specific LCI data when conducting environmental assessments of nano-enabled

463 products.
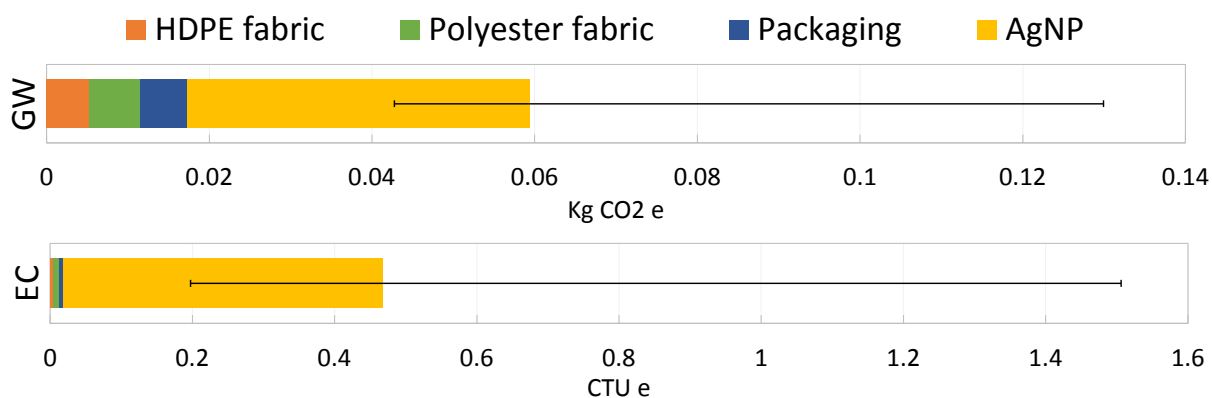
465 **Figure 3.** Absolute environmental impacts of bandage production shown for GWP and ecotoxicity. Error
466 bars demonstrate the high and low bounds for impacts depending on the production route. *Abbreviations*:
467 potential impact categories are global warming (GW) and ecotoxicity (EC).

468

Conclusion

470 AgNPs are projected to be an increasingly important material for a range of modern

471 technologies. Anticipatory analysis of potential environmental and health impacts is prudent,

472 while life cycle based results can uncover opportunities to improve efficiencies and lower

473   impacts. Here we look across all industrially important synthesis routes and compare LCA

474   results across them to explore what processes or inputs drive impacts for each route. Results are

475   presented scaled by the mass of nanoparticles produced and also, importantly, by nanoparticle

476   function, in this case antimicrobial efficiency. The choice between these two methods was

477   shown to change the rank order preference among synthesis methods for all environmental

478   impact categories considered.

479

Acknowledgments

Environmental Science: Nano Accepted Manuscript

Notes and References

484

485 1 A. A. Keller, S. McFerran, A. Lazareva and S. Suh, *J. Nanoparticle Res.*, 2013, **15**, 1–17.
486 2 J. Meesters, A. A. Koelmans, J. T. Quik, A. J. Hendriks and D. Van de Meent, *Environ. Sci. Technol.*,
487   2014.
488 3 M. E. Quadros, R. Pierson IV, N. S. Tulve, R. Willis, K. Rogers, T. A. Thomas and L. C. Marr, *Environ. Sci.*
489   *Technol.*, 2013, **47**, 8894–8901.
490 4 T. M. Benn and P. Westerhoff, *Environ. Sci. Technol.*, 2008, **42**, 4133–4139.
491 5 R. Kaegi, A. Voegelin, B. Sinnet, S. Zuleeg, H. Hagendorfer, M. Burkhardt and H. Siegrist, *Environ. Sci.*
492   *Technol.*, 2011, **45**, 3902–3908.
493 6 L. Hou, K. Li, Y. Ding, Y. Li, J. Chen, X. Wu and X. Li, *Chemosphere*, 2012, **87**, 248–252.
494 7 F. Gottschalk and B. Nowack, *J. Environ. Monit.*, 2011, **13**, 1145–1155.
495 8 E. S. Money, K. H. Reckhow and M. R. Wiesner, *Sci. Total Environ.*, 2012, **426**, 436–445.
496 9 S. A. Blaser, M. Scheringer, M. MacLeod and K. Hungerbühler, *Sci. Total Environ.*, 2008, **390**, 396–409.
497 10 N. C. Mueller and B. Nowack, *Environ. Sci. Technol.*, 2008, **42**, 4447–4453.
498 11 J. T. Quik, J. A. Vonk, S. F. Hansen, A. Baun and D. Van De Meent, *Environ. Int.*, 2011, **37**, 1068–1077.
499 12 L. M. Pasquini, S. M. Hashmi, T. J. Sommer, M. Elimelech and J. B. Zimmerman, *Environ. Sci. Technol.*,
500   2012, **46**, 6297–6305.
501 13 M. J. Eckelman and T. E. Graedel, *Environ. Sci. Technol.*, 2007, **41**, 6283–6289.
502 14 M. J. Eckelman, J. B. Zimmerman and P. T. Anastas, *J. Ind. Ecol.*, 2008, **12**, 316–328.
503 15 H. Sengul, T. L. Theis and S. Ghosh, *J. Ind. Ecol.*, 2008, **12**, 329–359.
504 16 T. Walser, E. Demou, D. J. Lang and S. Hellweg, *Environ. Sci. Technol.*, 2011, **45**, 4570–4578.
505 17 M. J. Eckelman, M. S. Mauter, J. A. Isaacs and M. Elimelech, *Environ. Sci. Technol.*, 2012, **46**, 2902–
506   2910.
507 18 L. Pourzahedi and M. J. Eckelman, *Environ. Sci. Technol.*, 2014, **49**, 361–368.
508 19 B. L. Cushing, V. L. Kolesnichenko and C. J. O'Connor, *Chem. Rev.*, 2004, **104**, 3893–3946.
509 20 J. A. Dahl, B. L. S. Maddux and J. E. Hutchison, *Chem. Rev.*, 2007, **107**, 2228–2269.
510 21 R. Hischier and T. Walser, *Sci. Total Environ.*, 2012, **425**, 271–282.
511 22 D. E. Meyer, M. A. Curran and M. A. Gonzalez, *J. Nanoparticle Res.*, 2011, **13**, 147–156.
512 23 B. A. Wender and T. P. Seager, *Anticipatory life cycle assessment of SWCNT-enabled lithium ion*
513   *batteries*, Nanotechnology for Sustainable Manufacturing, 2014.
514 24 P. Pati, S. McGinnis and P. J. Vikesland, *Environ. Eng. Sci.*, 2014, **31**, 410–420.
515 25 L. Pourzahedi and M. J. Eckelman, *Env. Sci Technol*.
516 26 A. Šileikaite, I. Prosycevas, J. Puiso, A. Juraitis and A. Guobiene, *Mater. Sci. Medžiagotyra*, 2006, **12**.
517 27 L. Mulfinger, S. D. Solomon, M. Bahadory, A. V. Jeyarajasingam, S. A. Rutkowsky and C. Boritz, *J.*
518   *Chem. Educ.*, 2007, **84**, 322.
519 28 R. H.-U. A. Slistan-Grijalva, *Phys. E-Low-Dimens. Syst. Amp Nanostructures - Phys. E*, 2005, **25**, 438–
520   448.
521 29 M. H. El-Rafie, M. E. El-Naggar, M. A. Ramadan, M. M. Fouda, S. S. Al-Deyab and A. Hebeish,
522   *Carbohydr. Polym.*, 2011, **86**, 630–635.
523 30 M. Zhou, Z. Wei, H. Qiao, L. Zhu, H. Yang and T. Xia, *J. Nanomater.*, 2009, **2009**, 3.
524 31 J. F. Pierson, D. Wiederkehr and A. Billard, *Thin Solid Films*, 2005, **478**, 196–205.
525 32 B. Nowack, H. F. Krug and M. Height, *Environ. Sci. Technol.*, 2011, **45**, 1177–1183.
526 33 F. H. Verhoff and J. E. Spradlin, *Biotechnol. Bioeng.*, 1976, **18**, 425–432.
527 34 V.-N. Tariq, L. A. J. Stefani and A. C. Butcher, *Biochem. Educ.*, 1995, **23**, 145–148.
528 35 T. M. Tolaymat, A. M. El Badawy, A. Genaidy, K. G. Scheckel, T. P. Luxton and M. Suidan, *Sci. Total*
529   *Environ.*, 2010, **408**, 999–1006.

Environmental Science: Nano Accepted Manuscript

530　36 K. C. Song, S. M. Lee, T. S. Park and B. S. Lee, *Korean J. Chem. Eng.*, 2009, **26**, 153–155.
531　37 N. Drogat, R. Granet, V. Sol and P. Krausz, *Nanoscale Res. Lett.*, 2010, **5**, 566–569.
532　38 U. D. of Health, H. Services and others, *Natl. Toxicol. Inf. Program Natl. Libr. Med. Bethesda Md*,
533　　　1993.
534　39 A. Slistan-Grijalva, R. Herrera-Urbina, J. F. Rivas-Silva, M. Avalos-Borja, F. F. Castillon-Barraza and A.
535　　　Posada-Amarillas, *Phys. E Low-Dimens. Syst. Nanostructures*, 2005, **25**, 438–448.
536　40 G. Carotenuto, G. P. Pepe and L. Nicolais, *Eur. Phys. J. B-Condens. Matter Complex Syst.*, 2000, **16**, 11–
537　　　17.
538　41 J. Li, J. Zhu and X. Liu, *Dalton Trans.*, 2014, **43**, 132–137.
539　42 S. Budavari, M. J. O'neil, A. Smith and P. E. Heckelman, 1989.
540　43 D. Hebbalalu, J. Lalley, M. N. Nadagouda and R. S. Varma, *Acs Sustain. Chem. Eng.*, 2013, **1**, 703–712.
541　44 A. Hebeish, M. H. El-Rafie, M. A. El-Sheikh and M. E. El-Naggar, *J. Nanotechnol.*, 2013, **2013**.
542　45 D. H. James and W. M. Castor, *Kirk-Othmer Encyclopedia of Chemical Technology*, John Wiley & Sons:
543　　　New York, 2011.
544　46 J. Chen, G. Lu, L. Zhu and R. C. Flagan, *J. Nanoparticle Res.*, 2007, **9**, 203–213.
545　47 C. Chazelas, J.-F. Coudert, J. Jarrige and P. Fauchais, *J. Eur. Ceram. Soc.*, 2006, **26**, 3499–3507.
546　48 M. Rai, A. Yadav and A. Gade, *Biotechnol. Adv.*, 2009, **27**, 76–83.
547　49 C. Marambio-Jones and E. M. Hoek, *J. Nanoparticle Res.*, 2010, **12**, 1531–1551.
548　50 J. M. Mäkelä, H. Keskinen, T. Forsblom and J. Keskinen, *J. Mater. Sci.*, 2004, **39**, 2783–2788.
549　51 Z. Wei, T. Xia, L. Bai, J. Wang, Z. Wu and P. Yan, *Mater. Lett.*, 2006, **60**, 766–770.
550　52 K. Varner, A. El-Badaway, D. Feldhake and R. Venkatapathy, *Us Environ. Prot. Agency Wash. Dc*, 2010,
551　　　**363**.
552　53 G. R. Tuttle, 2012.
553　54 J. Bare, *Clean Technol. Environ. Policy*, 2011, **13**, 687–696.
554　55 N. Vigneshwaran, R. P. Nachane, R. H. Balasubramanya and P. V. Varadarajan, *Carbohydr. Res.*, 2006,
555　　　**341**, 2012–2018.
556　56 A. Hebeish, M. E. El-Naggar, M. M. Fouda, M. A. Ramadan, S. S. Al-Deyab and M. H. El-Rafie,
557　　　*Carbohydr. Polym.*, 2011, **86**, 936–940.
558　57 M. Buşilă, V. Muşat, T. Textor and B. Mahltig, *Rsc Adv.*, 2015, **5**, 21562–21571.
559

Nanoparticle synthesis has been found in several life cycle assessments (LCAs) of Ag-NP containing products to be a large contributor of environmental impacts. Impacts are highly dependent on the synthesis route, yet several routes lack LCA data and/or results. Here we conduct and compare LCAs for all industrially important synthesis routes and identify critical inputs and synthesis steps, informing future process improvements. Impacts from the production of bulk silver were dominant for nearly every impact category, but with different patterns among routes. Results are presented on a mass basis as well as by antimicrobial efficiency, a novel approach. This work provides a transparent and general basis for the research community to model nano impacts in subsequent assessments of AgNP-enabled products.